AALBORG UNIVERSITY

DENMARK

Performance-degradation model for $Li_4Ti_5O_{12}$-based battery cells used in wind power applications

Stroe, Daniel Ioan; Swierczynski, Maciej Jozef; Stan, Ana-Irina; Teodorescu, Remus; Andreasen, Søren Juhl

Link to publication from Aalborg University

Performance-degradation model for $Li_4Ti_5O_{12}$-based battery cells used in wind power applications

D.I. Stroe, M. Swierczynski, A.I. Stan, R. Teodorescu, and S.J. Andreasen

Department of Energy Technology

Aalborg University, Denmark

E-mail: dis@et.aau.dk, mas@et.aau.dk, ast@et.aau.dk, ret@et.aau.dk, sja@et.aau.dk

Abstract—Energy storage systems based on Lithium-ion batteries have the potential to mitigate the negative impact of wind power grid integration on the power system stability, which is caused by the characteristics of the wind. This paper presents a performance model for a $Li_4Ti_5O_{12}/LiMO_2$ battery cell. For developing the performance model an EIS-based electrical modelling approach was followed. The obtained model is able to predict with high accuracy charge and discharge voltage profiles for different ages of the battery cell and for different charging/discharging current rates. Moreover, the ageing behaviour of the battery cell was analysed for the case of accelerated cycling ageing with a certain mission profile.

Index Terms—Lithium-ion battery, Performance model, Electrochemical Impedance Spectroscopy, Degradation.

I. INTRODUCTION

Future wind power plants (WPPs) are intended to function like todays conventional power plants seen from the transmission system perspective, by complying with the grid codes and providing a variety of ancillary services (e.g. inertia, primary frequency regulation, and forecast accuracy improvement). This will become possible by energy storage (ES) integration in the so-called virtual power plants (VPP) - ES + WPP. The ES system will act similar to a power and energy buffer and thus, the output of the virtual power plant will become more controllable, predictable and less variable [1].

Lithium-ion (Li-ion) batteries based on $Li_4Ti_5O_{12}$ (LTO) chemistry represent promising candidates for grid integration with WPPs due to their properties which include: high cycling stability, high rate charge/discharge capability, and high thermal stability in both charge and discharge state [2].

Developing performance models for Li-ion batteries and investigation of their ageing behaviour represents a key issue for the reliable integration of the battery in VPPs. In this paper, a performance model for LTO battery cells is developed based on measurements performed during an accelerated cycling ageing process. Since ageing tests under real operation conditions are extremely time consuming, accelerated ageing tests are usually preferred and extrapolation to real operation conditions is performed. The developed performance model is able to predict charge and discharge voltage characteristics for different C-rates and Ages (expressed as number of cycles at a certain DOD). Moreover, the ageing behaviour of the tested LTO battery cell is analysed in terms of capacity fade and changes of the Nyquist plots obtained from Electrochemical Impedance Spectroscopy (EIS) measurements.

TABLE I
VARIOUS CHEMISTRIES OF LI-ION BATTERIES AND THEIR CHARACTERISTICS (BASED ON [5]).

Chmiestry Anode/Cathode	Cell Voltage Max/Nominal [V]	Energy Density [Wh/kg]	Cycle life at 100% DOD	Thermal Stability
Graphite/ NiCoMnO$_2$	4.2/3.6	$100 - 170$	$2000 - 3000$	fairly stable
Graphite/ Mn spinel	4.0/3.6	$100 - 120$	1000	fairly stable
Graphite/ NiCoAlO$_2$	4.2/3.6	$100 - 150$	$2000 - 3000$	least stable
Graphite/ LiFePO$_4$	3.6/3.2	$90 - 115$	> 3000	stable
Li$_4$Ti$_5$O$_{12}$/ Mn spinel	2.8/2.3	$60 - 75$	> 5000	most stable

II. $LI_4TI_5O_{12}$ BATTERIES FOR WIND POWER APPLICATIONS

Li-ion batteries are seen as the key technology for the e-mobility sector and they emerge as the ES technology of the future for short and medium-time grid support applications. However in the later mentioned sector, the Li-ion technology is still in the demonstration stage [3].

There are many Li-ion battery chemistries available on the market, each with its specific electrical and economical characteristics. Latelly, a lot of effort was dedicated to the improvement of the Li-ion batteries chemistries by proposing new cathode and anode materials, and also by controlling the size of particles, their structure and morphology [4]. Consequently, choosing the proper Li-ion battery technology for integration with wind power plants is difficult.

The characteristics of the most popular Li-ion battery cell chemistries are summarized in Table I. Long cycle-life (at partial charge/discharge) is one of the most important demands in selecting batteries for wind power applications. Hence the utilization in wind power applications of Li-ion batteries based on Graphite/LiFePO$_4$ and $Li_4Ti_5O_{12}/LiMO_2$ becomes attractive even though their electrical performances are lower compared to the ones of graphite/LiMO$_2$ based batteries.

In this work a Li-ion pouch cell with the nominal capacity of 50 Ah and a nominal voltage of 2.3 V was used. The anode of the cell consists of $Li_4Ti_5O_{12}$ as active material while the cathode consists of LiCoO$_2$. In the followings, the cell with the aforementioned characteristics and chemistry will be simply called LTO battery cell.
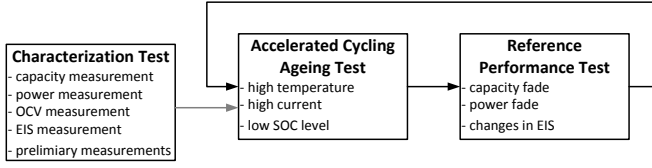
Fig. 1.   Accelerated ageing procedure for the LTO battery cell.

III. EXPERIMENTAL

The tests, to which the present LTO battery cell was subject to, were part of a selection procedure of the most suitable battery candidate for integration with VPPs. For more details about the aforementioned selection procedure the reader is referred to [6]. In order to obtain a fast degradation of the cells and to observe their ageing behaviour, accelerated ageing tests are necessary. The procedure which was followed to test the LTO battery cell is composed from three phases that are presented in Figure 1; these three phases are briefly described in the upcoming sections.

A. Characterization Test

During the characterization stage the LTO cell was subject to preliminary measurements, capacity, power, efficiency, open-circuit voltage as well as EIS measurements. The characterization of the cell was performed at different temperatures and considering different currents (C-rates). The results obtained during this stage are extensively presented in [7].

B. Accelerated Cycling Ageing Test

To obtain a fast degradation, the cell was cycled at high temperature (50 $\pm 2^oC$) by using high currents (200 A charging/discharging). Since long cycle lifetime at partial charge/discharge is required in many grid support applications, the cycling tests interval was chosen between 10 and 30% SOC as mentioned in [6]. The accelerated cycling ageing test was performed for a period of 4 weeks or 6500 partial charging/discharging cycles. After each week (1625 cycles) the accelerated cycling test was stopped for performing reference performance tests (RPTs) and resumed immediately after.

C. Reference Performance Test

In order to check the status of the LTO battery cell and to analyse its ageing behaviour, periodically RPTs were performed. During each RPT the following measurements were carried out:

A. capacity measurements; determination of the cell capacity during charging and discharging by applying three different C-rates (1, 2, and 4C-rate);

B. power measurements; determination of the cell power capability at 1, 2, and 4C for different SOC values;

C. EIS measurements; determination of the cell Nyquist characteristic for the 0 100% SOC interval with a 10% SOC resolution.

All the RPTs were performed at 25^oC, which represents the standard operating temperature of Li-ion batteries in stationary applications.

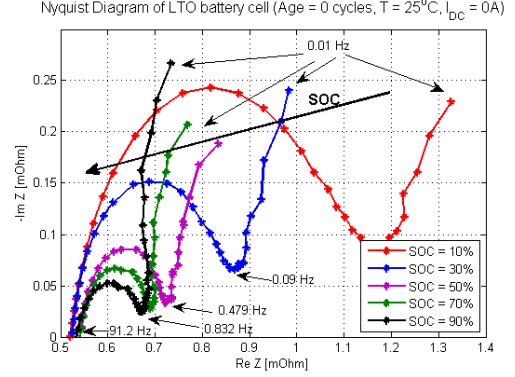| Age	Charged Capacity [Ah]			Discharged Capacity [Ah]		
	1C	2C	4C	1C	2C	4C
BOL	54.97	54.74	54.75	54.72	52.99	51.12
1675 cycles	53.11	54.91	53.54	54.14	53.61	52.15
3250 cycles	53.04	54.39	52.96	53.21	52.90	51.48
4875 cycles	49.28	51.14	50.76	50.77	50.65	49.90
6500 cycles	49.02	50.53	50.42	50.33	50.34	49.71

Fig. 2.   Measured impedance spectra of the LTO battery cell for different SOCs at 25^oC.

The measured charged and discharged capacity of the tested battery cell at different ages and for different currents are summarised in Table II. As expected, the discharged capacity of the cell is decreasing with increasing age for all the considered current rates. Moreover, it was observed that there exists a trend in the dependence of cell's discharged capacity on current rate with increasing Age.

Results of the EIS measurement performed during RPTs are presented in Figure 2 and Figure 3. The EIS measurements were performed at 25^oC and for SOCs between 0 and 100% with a 10% SOC increment. All the measurements were performed in the frequency range of 10 kHz 0.01 Hz with no DC-offset current.
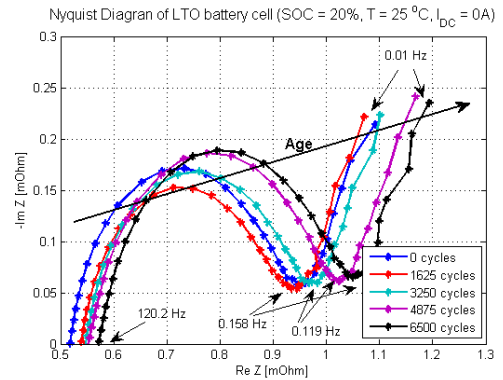

Fig. 3.   Measured impedance spectra of the LTO battery cell for different ages at 25^oC and 20% SOC.

As it may be observed form Figure 2, there is a relatively small dependence of the ohmic resistance on the SOC; however, an increase of the charge transfer semi circles
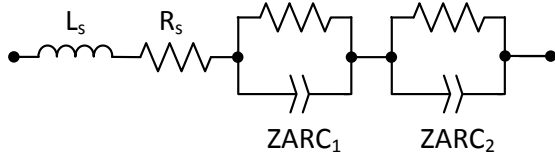
Fig. 4. Equivalent electrical circuit based on ZARC elements used for fitting the measured impedance spectra of the battery cell.

Fig. 5. Measured and fitted impedance spectra of the LTO battery cell.

was observed for small SOCs. On the other hand, Figure 3 illustrates that the ohmic resistance shows a strong dependence on the Age, while the effect of the same factor on the charge transfer semi circles and diffusion is limited.

IV. PERFORMANCE MODELLING

In order to obtain the performance model of a Li-ion battery cell, different approaches can be followed as described in the literature [8]. These approaches differ from each other from their degree of complexity point of view and from the modelling purpose point of view. Electrical performance models are considered by many researchers as a trade-off solution between electrochemical models and mathematical models because they involve moderate modelling complexity while offering relative high accuracy. The main drawback of these models is represented by their lack of accuracy if extrapolated to other material combinations or cell designs [9].

A. Modelling Approach

The electrical performance modelling approach used in this work to model the performance behaviour of the considered LTO cell is based on the EIS technique. In comparison to the DC pulse-based modelling approach, the chosen method shows several advantages which are extensively discussed in [10], [11].

The data obtained from EIS measurements were analysed using a standard procedure. In most of the cases, these data are presented in form of Nyquist plots, as shown in Figure 2. For all the considered cases (all SOCs and Ages) the measured Nyquist plots were curve fitted using a complex non-linear least square algorithm and a state-of-the-art equivalent electrical circuit based on ZARC elements [11]; the schematic of this equivalent electrical circuit (EEC) is presented in Figure 4. A comparison between measured and fitted/simulated EIS data is presented in Figure 5.

After fitting the EIS curves for all the measured SOCs and Ages, the dependence of the EEC parameters on the afore-mentioned factors was obtained. These dependencies were expressed as look up tables and used to build the performance model for the LTO battery cell. For exemplification, Figure 6 illustrates the behaviour of the R_s parameter for different SOCs and Ages.

The performance model was developed based on the block diagram presented in Figure 7. The input parameters of the model are the cell current, the initial SOC and the age of the cell (given in number of cycles). The performance model is intended to work only at a temperature equal to 25^oC, which
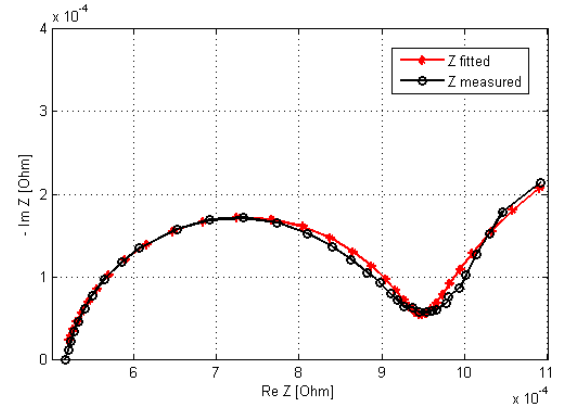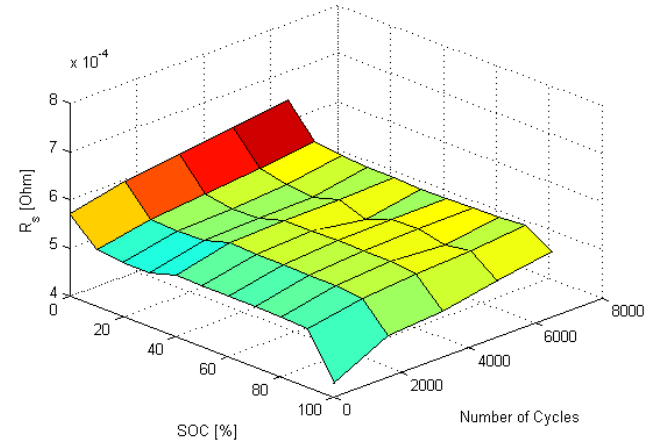

Fig. 6. Dependence on Age and SOC of the R_s parameter.

represents the working temperature of Li-ion batteries in wind power applications. The output of the performance model is the battery voltage.

The capacity of the battery cell was implemented as a tree-dimensional look-up tables, dependent on C-rate and Age, while its open-circuit voltage and all the EEC parameters were implemented as three-dimensional look-up tables, dependent on SOC and Age. The actual SOC was determined by integrating the cell current I_{Bat}, and it was always related to the measured cell capacity at the considered Age.

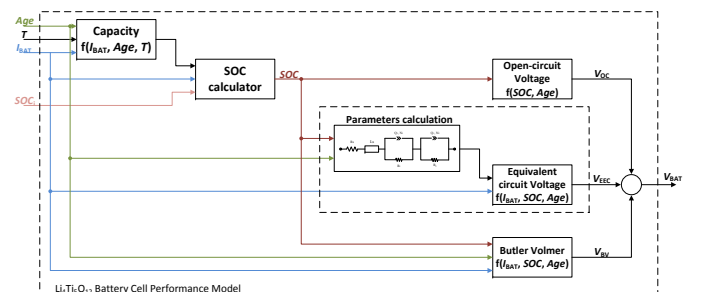Since all EIS measurements were performed without ap-

Fig. 7. Block diagram of the LTO battery cell performance model.

plying a DC-offset current, the effect of the current on the cell overvoltage was unknown. In order to overcome this limitation, the approximation for large currents of the Butler-Volmer equation (see equation 2) was used [12].

$$V_{BV} = \frac{R \cdot T}{\alpha \cdot F} \ln \left(\left| \frac{I_{Bat}}{A \cdot i_0} \right| \right) \tag{1}$$

where, R is the universal gas constant, T is the temperature, α is the symmetry factor, F is the Faraday constant, A is the active surface of the electrode, and i_0 is the exchange current density.

The battery cell voltage was obtained by summing the open-circuit voltage (V_{oc}) with the overvoltage contributions of the EEC (V_{EEC}) and Butler-Volmer:

$$V_{Bat} = V_{oc} + V_{EEC} + V_{BV} \tag{2}$$

B. Results

The developed LTO battery cell performance model was verified for different charging and discharging voltage profiles measured in the laboratory; at different ages (BOL, 1625 cycles, 3250 cycles, 4875 cycles and 6500 cycles) and considering different C-rates (1C, 2C, and 4C). The accuracy of the proposed model was quantified using the coefficient of determination R^2 that is defined as:

$$R^2 = 1 - \frac{\sum\limits_{SOC=0}^{SOC=100} (V_{MODEL}(SOC) - V_{LAB}(SOC))^2}{\sum\limits_{SOC=0}^{SOC=100} \left(V_{MODEL}(SOC) - \overline{V}_{LAB}(SOC)\right)^2} \tag{3}$$

A value of R^2 closer to 1 indicates a higher accuracy of the developed model. In Figure 8 and Figure 9, there are presented comparisons between predicted (modelled) and measured discharge voltage profiles, for different currents, at BOL and after 6500 cycles. It can be observed that the model is able to predict with high accuracy the cell voltage for the majority of the SOC interval. Small inaccuracies are observed for SOCs higher than 90% which can be associated with the variation for high SOCs of the symmetry factor (the symmetry factor was set constant for all SOCs at 0.5).

Figure 10 and Figure 11 show the verification of the developed performance model for predicting charge and discharge voltage profiles, at different ages, for 1C-rate current. The predicted voltage profiles show again good agreement with laboratory measured voltage profiles.

Table III summarizes the R^2 values obtained for all the verified cases. To conclude, the performance model developed for the LTO battery cell provides good results being able to predict with accuracy charge/discharge voltage profiles for different Ages and different currents, for a 25^oC operating temperature.
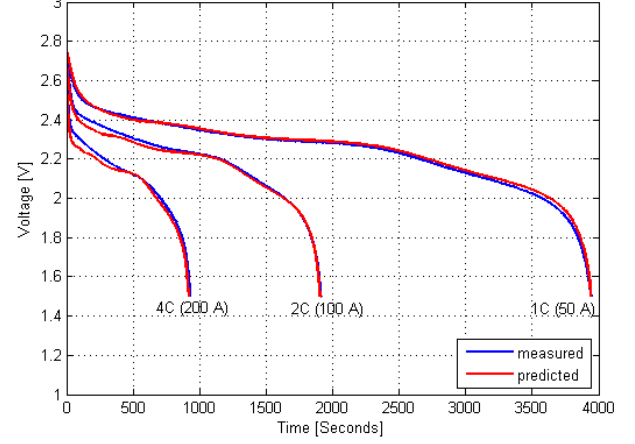

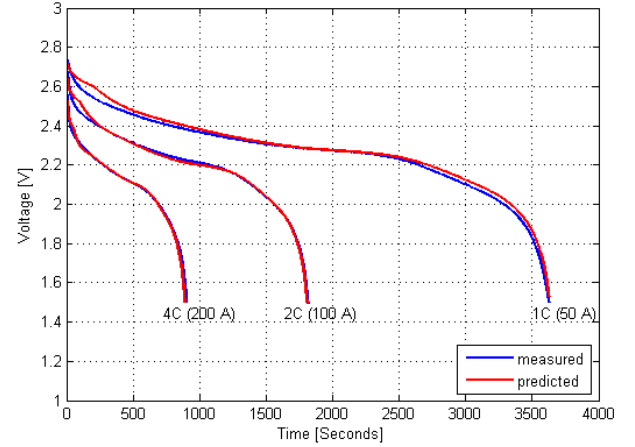Fig. 8. Predicted and measured discharge voltage profiles, for different currents at BOL.

Fig. 9. Predicted and measured discharge voltage profiles, for different currents after 6500 cycles.
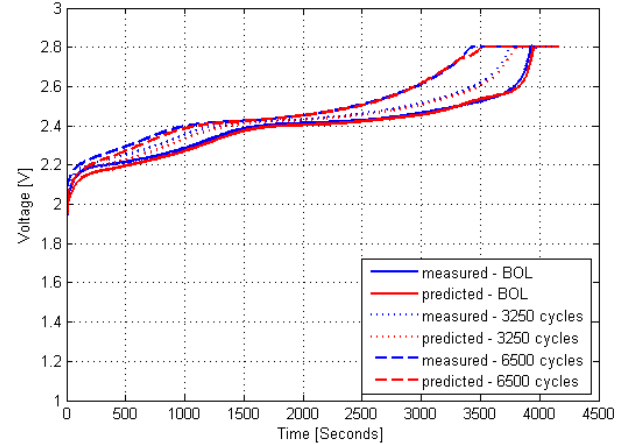

Fig. 10. Predicted and measured charge voltage profiles at different ages for 1C-rate (50A).
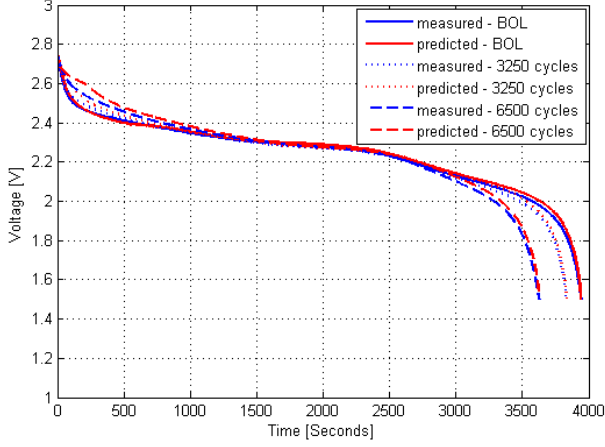
Fig. 11. Predicted and measured discharge voltage profiles at different ages for 1C-rate (50A).

TABLE III
R^2 COEFFICIENT OBTAINED FROM COMPARISONS OF THE MEASURED AND PREDICTED VOLTAGE PROFILES FOR DIFFERENT OPERATING CONDITIONS.

Age	Charge			Discharge		
	1C	2C	4C	1C	2C	4C
BOL	0.992	0.998	0.993	0.996	0.991	0.969
1675 cycles	0.990	0.985	0.971	0.978	0.993	0.974
3250 cycles	0.991	0.993	0.990	0.991	0.995	0.985
4875 cycles	0.990	0.985	0.930	0.983	0.994	0.969
6500 cycles	0.993	0.978	0.976	0.987	0.994	0.990

V. CYCLING AGEING RESULTS

During the four weeks of accelerated cycling ageing tests, the degradation of the LTO battery cell was monitored. Usually, the degradation of the Li-ion battery cells results in capacity fade, power fade, dc resistance increase, and changes in the EIS plots. In the upcoming sections the degradation of the battery form the point of view capacity fade and changes in the EIS plots is discussed.

A. Capacity Fade

The capacity of the LTO battery cell decreased with 8.03% during the first four weeks of the accelerated cycling ageing tests. Figure 12 presents the measured values of the capacity fade after each week of tests and an extrapolation until the end-of-life (EOL); 20% capacity drop was considered as EOL criterion.

Since the measured capacity fade reflects the degradation of the LTO cell's characteristics only for the first four weeks of the accelerated cycling tests, and not until the EOL, a precise extrapolation of the cell's capacity fade characteristic is difficult. It was found that the relation given in (4) describes well the capacity fade behaviour of the cell and matches the best the cell's datasheet.

$$C_{fade} = 0.05495 \cdot NC^{0.55} \tag{4}$$

where C_{fade} represents the capacity fade in % and NC represents the number of cycles for the SOC interval 10-30-10%. According to (4), the cell is able to deliver approximately
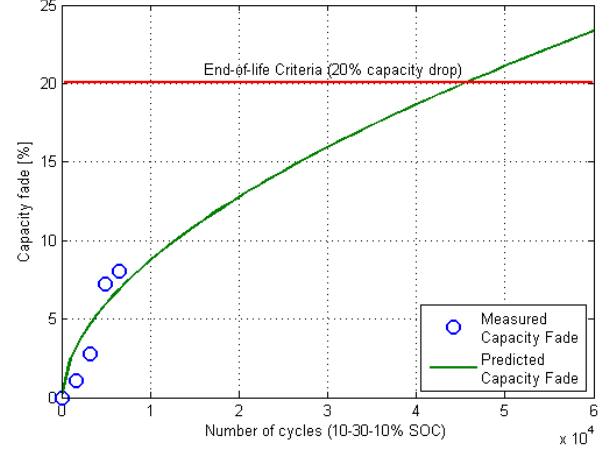

Fig. 12. Extrapolation of the capacity fade characteristic until EOL criterion.
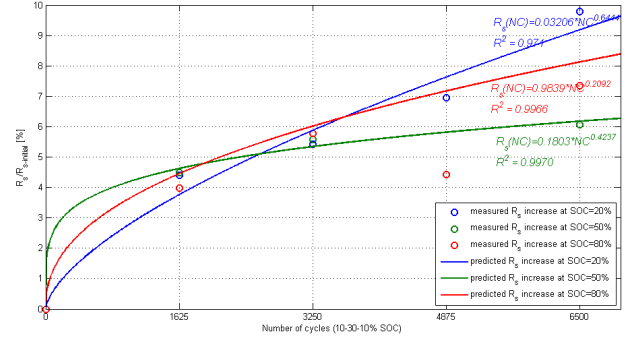

Fig. 13. Effect of the age on the value of R_s for different SOCs.

45 340 cycles (T = $50^{o}C$, SOC = 10-30-10%) until it will reach the predefined EOL criterion.

Few information is available on literature about the ageing mechanisms in Li-ion battery cells with LTO-based anodes. As mentioned in [13], LTO-based anodes cells do not form a SEI. Consequently it is expected that the rate of ageing at the anode side of these cells to be reduced or even totally eliminated. Thus, it is possible that the capacity fade of these cells to only result from the processes at the cathode side, e.g. metal dissolution and phase transitions [14].

B. Changes in EIS plots

During the accelerated ageing cycling tests, changes in the EIS plots were observed. An example is given in Figure 3 where Nyquist curves are plotted for SOC = 20% at different Ages. It can be observed that with the increasing age, the ohmic resistance is increasing also. On the other hand, the effect of Age on the charge transfer semi circles and diffusion is limited. The same ageing behaviour was obtained for the majority of SOCs. Moreover, by analysing the values of the parameters of the EEC, which were obtained from fitting the measured impedance spectra, only for R_s a clear trend was observed. Figure 13 illustrates the dependence on age (number of cycles) of the R_s parameter at three different SOCs.

By analysing Figure 13, it can be concluded that the increase of the R_s values for increased age is more pronounced for

close to extreme SOCs (e.g. 20% and 80%) than for middle SOCs (e.g. 50%). Since no measurements with a reference electrode were performed, it cannot be distinguished if the changes on the EIS curves with increasing age are caused by the processes at the anode side or at the cathode side.

VI. CONCLUSIONS

Li-ion batteries based on LTO anodes are suitable for being used in ES systems connected with WPPs due to their characterisics: high cycling stability, high rate charge/discharge capability, and high thermal stability in both charge and discharge state.

In this paper a performance model for LTO battery cells was proposed. The developed performance model was obtained following an EIS-based electrical modelling approach. The parameters of the EEC and the open-circuit voltage were implemented as three-dimensional look-up tables, dependent on age and SOC, while the capacity of the battery cell was implemented as a three-dimensional look-up table, dependent on age and C-rate. The obtained performance model was verified by comparing laboratory measurements with simulation results. It was found that the model predicts with accuracy charge and discharge voltage profiles for different ages and different currents, for a 25^oC operating temperature.

The ageing behaviour of the LTO battery cell was analysed from the point of view of capacity fade and changes in the EIS plots. Even though the estimation of the capacity fade until the EOL is difficult when only few measurements points are available, a good correlation with the data sheet values was obtained. Moreover, from the EIS measurements obtained in the first four weeks of accelerated cycling tests, it was found that mainly the ohmic resistance of the EEC is age-dependent.

REFERENCES

[1] C. Rasmussen, "Energy storage for improvement of wind power characteristics," in *2011 IEEE PowerTech Trodheim, Norway*, June 2011, pp. 1–8.

[2] B. Scrosati and J. Garche, "Lithium batteries: Status, prospects and future," *Journal of Power Sources*, vol. 195, pp. 2419–2430, 2010.

[3] D. Rastler, "Electricity energy storage technology options. a white paper primer on applications, costs, and benefits," EPRI-DOE, Tech. Rep., December 2010.

[4] B. Dunn, H. Kamath, and J. Tarasacon, "Electrical energy storage for the grid: A battery of choices," *Science*, vol. 6058, pp. 928–935, November 2011.

[5] A. Burke and M. Miller, "Performance charactersitics of lithium-ion batteries of various chemistries for plug-in hybrid vehicles," in *EVS24*, 13-16 May 2009.

[6] M. Swierczynski, D. Stroe, A. Stan, R. Teodorescu, and H. Vikelgaard, "Selection and impedance based model of a lithium ion battery technology for integration with virtual power plant," in *EPE Joint Wind Energy and T&D Chapters Seminar*, 28-29 June 2012.

[7] M. Swierczynski, D. Stroe, A. Stan, R. Teodorescu, and D. Sauer, "Performance modeling of lithium titanate oxide (li4ti5o12) and lithium iron phosphate (lifepo4) batteries for integration with wind power plants," (to be published).

[8] M. Chen and G. Rincon-Mora, "Accurate electrical battery model capable of predicting runtime and i-v performance," *IEEE Transactions on Energy Conversion*, vol. 21, pp. 504–511, June 2006.

[9] D. Sauer and H. Wenzl, "Comparison of different approaches for lifetime prediction of electrochemical systemsusing lead-acid batteries as example," *Journal of Power Sources*, vol. 176, pp. 534–546, February 2008.

[10] S. Buller, M. Thele, R. De Donker, and E. Karden, "Impedance-based non-linear dynamic battery modeling for automotive applications," *Journal of Power Sources*, vol. 113, pp. 422–430, January 2003.

[11] D. Andre, M. Meiler, K. Steiner, C. Wimmer, T. Soczka-Guth, and D. Sauer, "Characterization of high-power lithium-ion batteries by electrochemical impedance spectroscopy. i. experimental investigation," *Journal of Power Sources*, vol. 196, pp. 5334–5341, June 2011.

[12] D. Andre, M. Meiler, K. Steiner, H. Waltz, T. Soczka-Guth, and D. Sauer, "Characterization of high-power lithium-ion batteries by electrochemical impedance spectroscopy. ii: Modelling," *Journal of Power Sources*, vol. 196, pp. 5349–5356, June 2011.

[13] J. McDowall, "Understanding li-ion technology," in *BATTCON*, 2008.

[14] J. Vetter, P. Novak, M. Wagner, C. Veit, K. Mller, J. Besenhard, M. Winter, M. Wohlfahrt-Mehrens, C. Vogler, and A. Hammouche, "Ageing mechanisms in lithium-ion batteries," *Journal of Power Sources*, vol. 147, pp. 269–281, 26-30 2005.